The sigma-1 receptor modulates dopamine transporter conformation and cocaine binding and may thereby potentiate cocaine self-administration in rats

Received for publication, December 23, 2016, and in revised form, May 10, 2017 Published, Papers in Press, May 11, 2017, DOI 10.1074/jbc.M116.774075

Weimin Conrad Hong[‡1], **Hideaki Yano**[§], **Takato Hiranita**[§], **Frederick T. Chin**[¶], **Christopher R. McCurdy**[‖], **Tsung-Ping Su**[§], **Susan G. Amara**[**], **and Jonathan L. Katz**[§]

From the [‡]*Department of Pharmaceutical Sciences, Butler University, Indianapolis, Indiana 46208,* [§]*Intramural Research Program, National Institute on Drug Abuse, Baltimore, Maryland 21224,* [¶]*Molecular Imaging Program at Stanford (MIPS), Department of Radiology, Stanford University, Stanford, California 94305, the* [‖]*Department of Medicinal Chemistry, College of Pharmacy, University of Florida, Gainesville, Florida 32610, and the* [**]*Laboratory of Molecular and Cellular Neurobiology, National Institute of Mental Health, Bethesda, Maryland 20892*

Edited by F. Anne Stephenson

The dopamine transporter (DAT) regulates dopamine (DA) neurotransmission by recapturing DA into the presynaptic terminals and is a principal target of the psychostimulant cocaine. The sigma-1 receptor (σ_1R) is a molecular chaperone, and its ligands have been shown to modulate DA neuronal signaling, although their effects on DAT activity are unclear. Here, we report that the prototypical σ_1R agonist (+)-pentazocine potentiated the dose response of cocaine self-administration in rats, consistent with the effects of the σR agonists PRE-084 and DTG (1,3-di-*o*-tolylguanidine) reported previously. These behavioral effects appeared to be correlated with functional changes of DAT. Preincubation with (+)-pentazocine or PRE-084 increased the B_{max} values of [^{3}H]WIN35428 binding to DAT in rat striatal synaptosomes and transfected cells. A specific interaction between σ_1R and DAT was detected by co-immunoprecipitation and bioluminescence resonance energy transfer assays. Mutational analyses indicated that the transmembrane domain of σ_1R likely mediated this interaction. Furthermore, cysteine accessibility assays showed that σ_1R agonist preincubation potentiated cocaine-induced changes in DAT conformation, which were blocked by the specific σ_1R antagonist CM304. Moreover, σ_1R ligands had distinct effects on σ_1R multimerization. CM304 increased the proportion of multimeric σ_1Rs, whereas (+)-pentazocine increased monomeric σ_1Rs. Together these results support the hypothesis that σ_1R agonists promote dissociation of σ_1R multimers into monomers, which then interact with DAT to stabilize an outward-facing DAT conformation and enhance cocaine binding. We propose that this novel molecular mechanism underlies the behavioral potentiation of cocaine self-administration by σ_1R agonists in animal models.

This work was supported by Butler University Faculty Startup Fund and Holcomb Research Award (to W. C. H.), National Institutes of Health Intramural Research Programs (to H. Y., T. H., T. P. S., S. G. A., and J. L. K.), Grant R37 DA007595 (to S. G. A.), and in part by Grants R01 DA023205 (to C. R. M.) and P20 GM104932 (to C. R. M.). C. R. M. and F. T. C. are co-inventors and patent holders of CM304. The content is solely the responsibility of the authors and does not necessarily represent the official views of the National Institutes of Health.

[1] To whom correspondence should be addressed: Dept. of Pharmaceutical Sciences, Butler University, PB351, 4600 Sunset Ave., Indianapolis, IN 46208. Tel.: 317-940-9580; Fax: 317-940-6172; E-mail: chong@butler.edu.

Upon synaptic release of dopamine (DA),[2] the dopamine transporter (DAT) recaptures DA into presynaptic terminals and regulates the intensity and duration of DA neurotransmission (1, 2). The DAT is a principal target of the abused psychostimulants, cocaine and methamphetamine. The abuse of and addiction to these drugs stem from their ability to inhibit DAT and elevate extracellular DA levels. Extensive characterization has shown that DAT function can be regulated by posttranslational modifications such as phosphorylation and by multiple interacting proteins (3–6). Recent breakthroughs in the X-ray crystal structure of the *Drosophila* DAT reveal that cocaine occupies the substrate-binding pocket in DAT while trapping the transporter in an outward-facing conformation (7).

The sigma receptor (σR) was initially proposed as a subtype of opioid receptors (8). After the molecular cloning of the sigma-1 receptor (σ_1R) subtype as a 25-kDa membrane protein (9), studies from several groups have shown that it is a molecular chaperone that can interact with and modulate the activity of a variety of client proteins, including ankyrin (10), potassium channels (11, 12), BiP (13), DA D_1 and D_2 receptors (14, 15), and opioid receptors (16). The crystal structure of σ_1R has recently been solved, showing a homotrimer with each protomer containing a single transmembrane domain (TM) and a cytoplasmic domain mediating ligand-binding and subunit multimerization (17).

σRs were shown to regulate midbrain DA neuronal firing and modulate DA release in earlier pharmacological studies (18, 19). Several σR ligands have been explored for their therapeutic potential in treating stimulant abuse (20, 21). A recent behavioral study showed that σ_1R agonists such as PRE-084 and 1,3-di-*o*-tolylguanidine (DTG), but not σ_1R antagonists, increased the potency of cocaine in a self-administration procedure (22). Furthermore, cocaine self-administration experi-

[2] The abbreviations used are: DA, dopamine; DAT, DA transporter; σR, sigma receptor; σ_1R, sigma-1 receptor; TM, transmembrane domain; DTG, 1,3-di-*o*-tolylguanidine; EXT, extinction; EAAT2, excitatory amino acid transporter-2; BRET, bioluminescence resonance energy transfer; GDN, glyco-diosgenin; PFO, perfluorooctanoic acid; ANOVA, analysis of variance; SPB, sucrose-phosphate buffer; FR, fixed-ratio; RLuc, *Renilla* luciferase; FH-σ_1R, FLAG-2 × His_8-σ_1R.

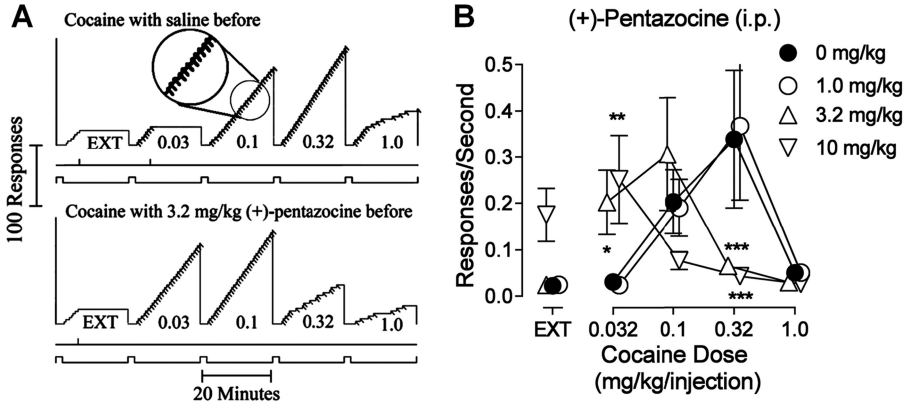

Figure 1. The σ_1R agonist (+)-pentazocine dose-dependently potentiated cocaine self-administration in rats. *A*, representative cumulative records of an individual subject responding showing patterns of self-administration in real time maintained by intravenous cocaine when each fifth-response produced an injection (fixed-ratio, or FR 5-response schedule). *Ordinates* show cumulative responses. *Abscissae* show time. The five 20-min self-administration components of each session are indicated by a *downward displacement of the lowest line below each record*. At the end of each component the cumulative-response curve reset to base. The preceding 2-min timeout periods are indicated by the *upward position of the lowest line of each record*. In the first component, each fifth response turned off the light-emitting diodes for 20 s but did not activate the infusion pump (*EXT*); in subsequent components, injections were also delivered with each fifth response (*diagonal marks on the cumulative record*) with doses (in mg/kg/injection) indicated. *Vertical marks on the event line below the cumulative curve* indicate responses on the *left* (inactive) lever. The encircled portion of the record in the third component is magnified to better show the temporal pattern of responding. Note the dose-dependent increase in responding up to the cocaine dose of 0.32 mg/kg/injection in the top record and the increases in responding at lower doses of cocaine after pretreatment with 3.2 mg/kg of (+)-pentazocine in the bottom record. In general, (+)-pentazocine affected overall rates without changes in the temporal pattern of responding. *B*, dose-effect curves of cocaine self-administration and the effect of (+)-pentazocine treatment. Each point represents the mean ± S.E. ($n = 6$) of response rates maintained during extinction (*EXT*, responses had no scheduled consequences) or under the FR5 schedule at the indicated cocaine doses/injection. *Asterisks* indicate significant effects of the doses of i.p. (+)-pentazocine (○, △, ▽) compared with saline pretreatment (●) as determined by two-way repeated measures ANOVA and Tukey post-hoc tests (*, $p < 0.05$; **, $p < 0.01$; ***, $p < 0.001$). Note that (+)-pentazocine rendered the subject more sensitive to cocaine dose.

ence induced self-administration of σ_1R agonists, an effect not likely mediated by changes of DA receptors (23, 24). In the present study we investigated the effects of σ_1R ligands on DAT function using behavioral, pharmacological, and biochemical methods. We present several lines of evidence supporting the hypothesis that interaction of σ_1R with DAT modulates the outward-facing conformation of DAT and facilitates cocaine binding to DAT. This molecular mechanism underscores a novel modulatory role of σ_1R on DA neurotransmission and suggests therapeutic potentials of σ_1R ligands in treating cocaine addiction.

Results

Rats with indwelling venous catheters were trained to self-administer cocaine using an established procedure in which each fifth press on a lever produced an injection. Lever-press responding maintained by cocaine injections was similar to that reported previously with cocaine or other more conventional reinforcers under similar schedules. A brief pause was followed by a sequence of five responses made in rapid succession producing the injection (Fig. 1*A*; *top panel*, see the *inset* for a magnified display of the micro-temporal pattern). Few if any responses were emitted on the inactive lever (*vertical marks on the line below cumulative curve*) or during the 2-min timeout periods (*lower event line displaced upward*) between successive components. In the extinction (EXT) component no injections were delivered, and response rates were low. As the dose of cocaine increased in successive components, response rates also increased. The highest rate of responding was obtained in the fourth component in which injections of 0.32 mg/kg were available (Fig. 1*A*, *top record*). When saline injections were available in the second through fifth components (data not shown), responses were never emitted at rates greater than those maintained in EXT. The average response rates were a bell-shaped function of cocaine dose (Fig. 1*B*, *filled symbols*). The maximum response rate averaging 0.339 (± S. E. 0.073) responses/s was obtained with a dose of 0.32 mg/kg/injection and was significantly greater than the rates averaging 0.023 (± S. E. 0.003) responses/s during EXT.

Pre-session intraperitoneal (i.p.) injection with (+)-pentazocine dose-dependently shifted the cocaine self-administration dose-effect curve leftward, without affecting maximum response rate (Fig. 1*B*). The lowest dose of (+)-pentazocine (1.0 mg/kg) was inactive, whereas doses of 3.2 and 10 mg/kg produced leftward shifts that approximated 3- and 10-fold, respectively. These changes were obtained without appreciable effects on the temporal patterns of responding (Fig. 1*A*, *bottom record*). The major difference in the performances after (+)-pentazocine or vehicle pretreatment were that the highest response rates were obtained at lower doses of cocaine after (+)-pentazocine. Two-way repeated measures analysis of variance (ANOVA) indicated a significant effect on response rate ($F_{4,60} = 5.60$; $p = 0.003$), with drug pretreatment dose and component (EXT and cocaine dose) as factors. Post-hoc Tukey comparisons indicated that response rates maintained at 0.32 mg/kg/injection of cocaine were significantly decreased by 3.2 and 10 mg/kg of (+)-pentazocine ($q = 5.78, 6.25$, respectively; p values <0.001). However, the low response rates at 0.032 mg/kg/injection of cocaine were increased by 10.0 mg/kg of (+)-pentazocine ($q = 4.66$; $p = 0.009$). Overall, after (+)-pentazocine pretreatment lower doses of cocaine maintained the highest responses rates compared with vehicle pretreatment. Such potentiating effects on cocaine self-administration by (+)-pentazocine were consistent with those produced by other σ_1R agonists (PRE-084 and DTG) in a previous report (22).

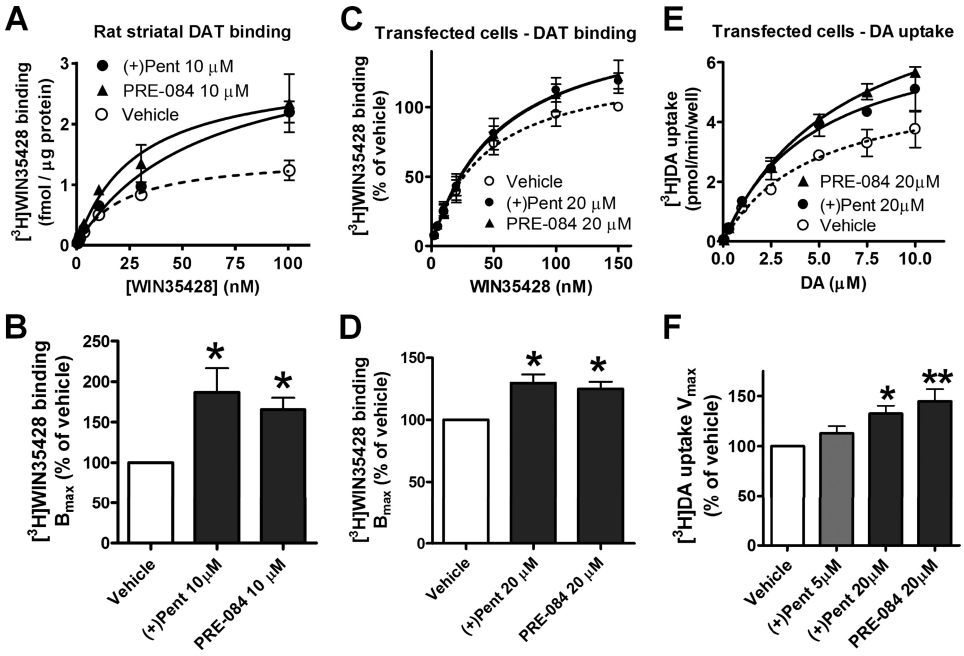

Figure 2. Regulation of DAT function by σ_1R agonists in native tissues and transfected cells. *A* and *B*, rat striatal slices were incubated with σ_1R agonists, washed, and homogenized to measure [^{3}H]WIN35428 binding. Shown are representative binding curves with triplicate samples (mean ± S.D.) and summarized B_{max} values (mean ± S.E., $n = 4–5$ experiments) in the *bar graph*. *C* and *D*, HEK293 cells transfected with DAT and σ_1R were incubated with σ_1R agonists, washed, and measured for [^{3}H]WIN35428 binding. Shown are representative binding curves with triplicate samples (mean ± S.D.) and summarized B_{max} values (mean ± S.E., $n = 3$ experiments) in the *bar graph*. *E* and *F*, HEK293 cells transfected with DAT and σ_1R were incubated with σ_1R agonists, washed, and measured for [^{3}H]DA uptake. Shown are representative results with triplicate samples (mean ± S.D.) and summarized V_{max} values (mean ± S.E., $n = 3$ - 5 experiments) in the *bar graph*. *, $p < 0.05$; **, $p < 0.01$, one-way ANOVA and post-hoc Dunnett's test, compared with vehicle. *(+)pent*, (+)-pentazocine.

The relation between cocaine self-administration and DAT function suggests that potentiation of cocaine self-administration by σ_1R agonists may involve modulation of DAT by these drugs. Because cocaine inhibits the DAT by direct binding, we tested the effects of σ_1R ligands on the binding of [^{3}H]WIN35428, a radiolabeled cocaine analog, in rat brain tissues with a high density of DAT. Freshly harvested rat striatal slices were incubated with σ_1R agonists, washed multiple times to remove residual drugs, then homogenized to measure binding the of [^{3}H]WIN35428. Specific binding was adjusted for variations of protein concentrations among treatment groups. After preincubation with 10 μM (+)-pentazocine or PRE-084, B_{max} values of [^{3}H]WIN35428 binding in striatal homogenates were significantly increased (mean ± S.E.: 187 ± 30% and 166 ± 15% of vehicle, respectively; Fig. 2, *A* and *B*), whereas K_i values were not substantially changed.

We further examined the effects of σ_1R agonists on DAT function in HEK293 cells co-transfected with DAT and σ_1R. Because cocaine preferentially binds to DAT in the outward-facing conformation (7), we reasoned that potential changes of DAT conformation and cocaine binding might be more easily unmasked under conditions of low extracellular Na^+, in which the conformational equilibrium of DAT is shifted toward the inward-facing state. We found that [^{3}H]WIN35428 binding was correlated with increasing extracellular Na^+ in a dose-dependent manner in these cells, and that although binding at 50 mM Na^+ was reduced to half that in normal Na^+ (150 mM), it still could be measured reliably (data not shown). Thus, cells were incubated with σ_1R ligands and subsequently assayed for DAT binding or substrate uptake in a buffer with 50 mM NaCl and 100 mM *N*-methyl-D-glucamine. Similar to results obtained using striatal tissues, there was a significant increase of [^{3}H]WIN35428 binding B_{max} in these cells pretreated with (+)-pentazocine or PRE-084 (130 ± 7% or 125 ± 6% of vehicle, respectively; Fig. 2, *C* and *D*) without substantial changes in K_i values. Similar effects of σ_1R agonists on DAT binding were observed in another cell line expressing HA-tagged DAT and Myc-tagged σ_1R (data not shown). Additionally, there was a significant increase of [^{3}H]DA uptake V_{max} values in cells pre-incubated with (+)-pentazocine or PRE-084 (133 ± 8% or 145 ± 12% of vehicle, respectively; Fig. 2, *E* and *F*) without substantial changes of K_m values.

As σ_1R has been shown to be a versatile molecular chaperone that can interact with multiple membrane proteins (25), we examined whether σ_1R could interact with neurotransmitter transporters. In HEK293 cells GST-tagged-σ_1R was co-expressed together with Myc-tagged-σ_1R, DAT, or the excitatory amino acid transporter-2 (EAAT2). When GST-σ_1R was affinity-purified from cell lysates by glutathione beads, a strong signal of Myc-σ_1R was observed, suggesting the existence of a robust constitutive interaction that facilitated the formation of multimers. Substantial signals from the DAT were also detected, whereas no signal of EAAT2 was detected despite its higher expression level (Fig. 3*A*). The bands detected for DAT corresponded to unglycosylated (~55 kDa), glycosylated (~80–90 kDa), and high molecular weight (M_r) oligomeric forms, suggesting that σ_1R likely interacts with DAT directly or indirectly in various cellular compartments, including those mature, glycosylated DAT on the cell surface. Furthermore, in cells co-transfected with σ_1R and DAT, σ_1R could be co-immunoprecipitated with DAT using DAT-specific antibody MAB369 but not with control IgG (Fig. 3*B*).

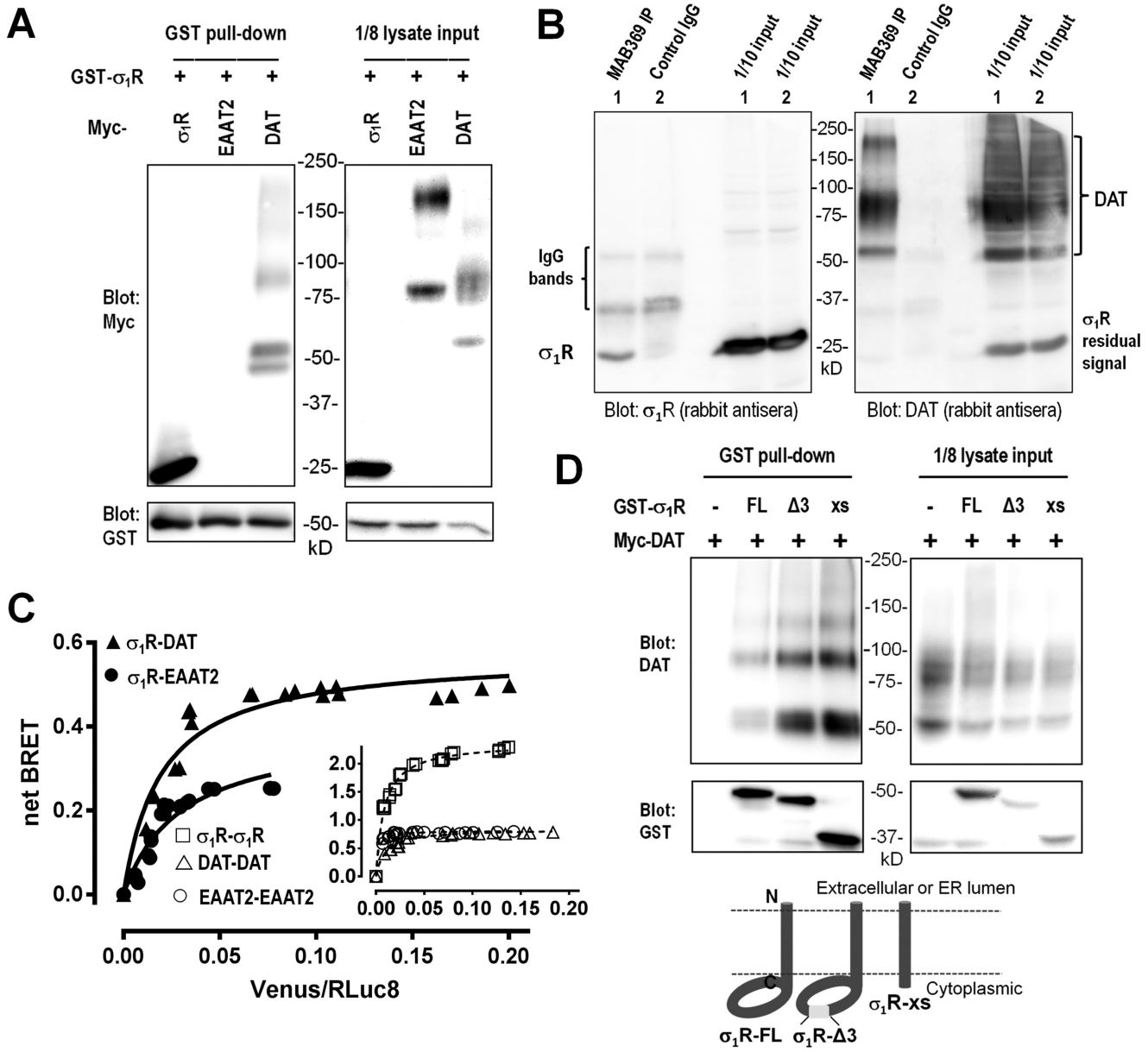

Figure 3. Interaction between DAT and σ_1R. *A*, DAT, but not EAAT2, was pulled down with GST-σ_1R in transfected HEK293 cells. Representative blots from five experiments are shown. Note in the pull-down sample the presence of unglycosylated, glycosylated, and oligomeric forms of DAT, with a possible partial degradation product (~45 kDa). *B*, co-immunoprecipitation of DAT and σ_1R in transfected HEK293 cells. DAT was immunoprecipitated (*IP*) by rat monoclonal antibody (MAB369) but not by normal rat IgG as control. *Left*, detection of σ_1R; *right*, membrane was reblotted to confirm enrichment of DAT. Antibodies raised from different species were used to minimize cross-reactivity to IgG proteins. *C*, molecular interaction between σ_1R and DAT measured by BRET. HEK 293T cells were transfected with a constant amount of the RLuc-fusion construct and increasing amounts of the Venus-fusion construct. Molecular interactions between σ_1R and DAT and between σ_1R and EAAT2 are compared by measuring the energy transfer between the two fusion protein partners: σ_1R-Rluc-Venus-EAAT2 (●) and σ_1R-Rluc-Venus-DAT (▲). Homomeric pairs for DAT, EAAT2, and σ_1R were used as controls: Rluc-EAAT2-Venus-EAAT2 (○), Rluc-DAT-Venus-DAT (△), σ_1R-Rluc - σ_1R-Venus (□). All data points were performed in triplicate (S.E. error bars were obscured by symbols). The $BRET_{max}$ values were calculated by nonlinear regression using a single-site saturation binding model. *D*, analysis of interaction domains on σ_1R with DAT. GST-tagged full-length (*FL*) σ_1R or C-terminal deletion variants (σ_1R-xs and σ_1R-Δ3) were co-transfected with Myc-tagged DAT. Stronger DAT signals were co-enriched with GST-σ_1 xs or Δ3 compared with GST-σ_1 FL (*upper panel*). The membrane was then blotted with antibodies against GST to confirm GST pulldown (*lower panel*).

The interaction between σ_1R and DAT was further verified in live cells using bioluminescence resonance energy transfer (BRET) method. Consistent with the results using GST pull-down assays, co-expression of σ_1R and DAT resulted in substantially higher $BRET_{max}$ signals than co-expression of σ_1R and EAAT2 (Fig. 3*C*, ▲ and ●, respectively), whereas DAT-DAT and EAAT2-EAAT2 interactions (Fig. 3*C*, *inset*, △ and ○, respectively) showed similar $BRET_{max}$ values, indicating that the difference between the $BRET_{max}$ between σ_1R-DAT and σ_1R-EAAT2 was significant. The σ_1R-σ_1R BRET pair exhibited the most robust signals (Fig. 3*C*, *inset*, □), confirming the multimerization of σ_1R, as shown in Fig. 3*A*.

Several splice variants of σ_1R display different lengths in their cytoplasmic domains, including one variant (GenBank™ NM_147157.2) lacking exon 3 (σ_1-Δ3) that encodes amino acids 119–149 and another (GenBank™ BC007839.2) that has a frameshift-induced early termination and deletion of amino acids 103–223 (σ_1R-xs). When GST-tagged σ_1R-Δ3 and σ_1R-xs

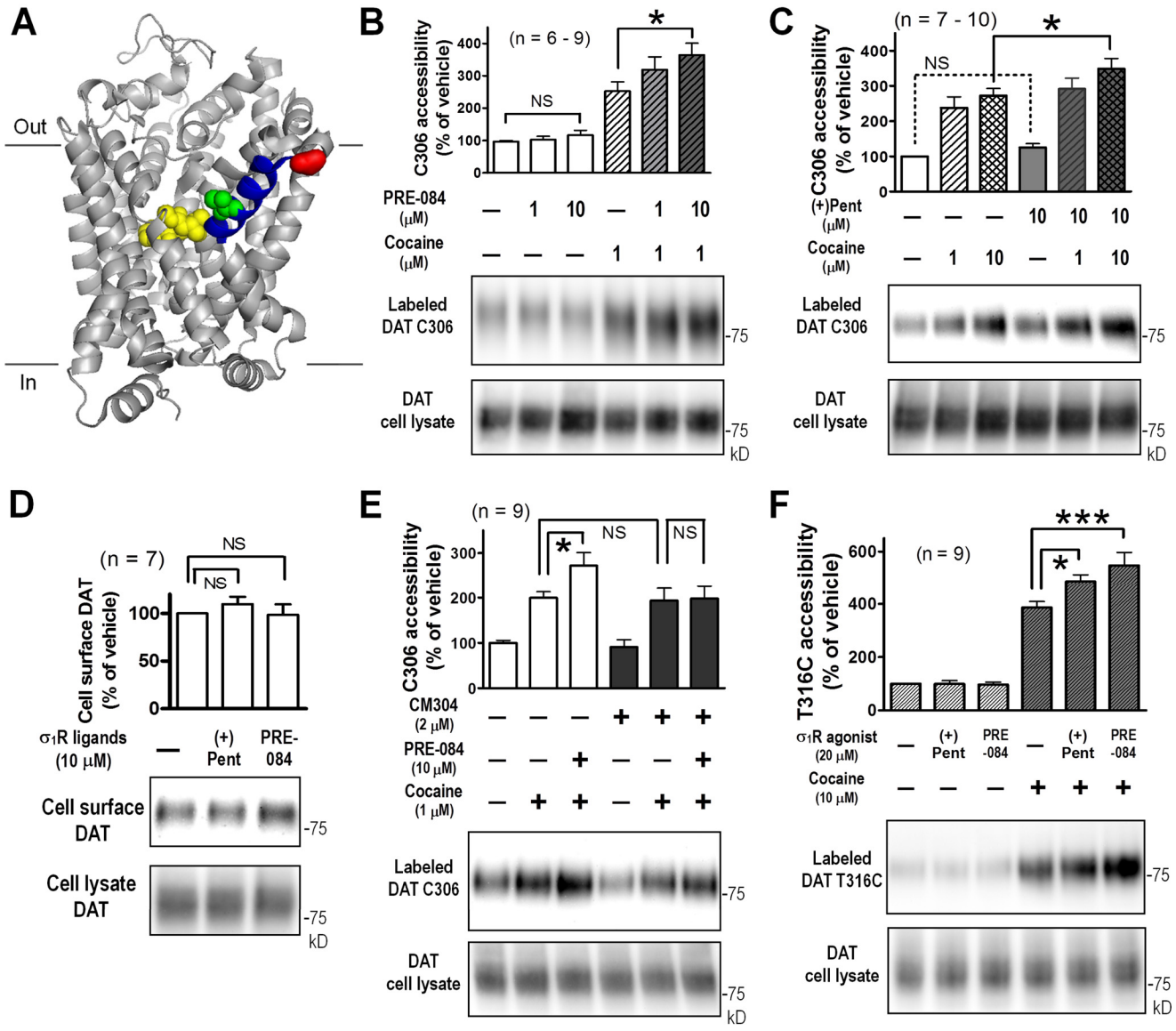

Figure 4. Modulation of DAT conformation by σ_1R agonists in the presence of cocaine. *A*, schematic of the *Drosophila* DAT structure with cocaine (*yellow*) bound (PDB 4XP4) (7). Highlighted positions corresponding to Cys-306 (*red*), Thr-316 (*green*), and TM6a (*blue*) in human DAT. Part of TM11 was omitted for clarity. *B* and *C*, potentiation of cocaine-induced accessibility changes of Cys-306 in DAT by σ_1R agonists. Transfected HEK293 cells expressing DAT and epitope-tagged σ_1R were preincubated with PRE-084 or (+)-pentazocine for 1 h at 37 °C, washed with PBSCM, and labeled with maleimide-PEG2-biotin at 4 °C for 45 min in the presence or absence of cocaine. Biotinylated proteins were enriched from cell lysates with NeutrAvidin beads, subjected to SDS-PAGE, and detected on immunoblot using DAT-specific antibodies (see details under "Experimental procedures"). *D*, σ_1R agonists did not change cell expression levels of DAT. Transfected cells were incubated with σ_1R drugs for 1 h at 37 °C, washed with PBSCM, and labeled with sulfo-NHS-SS-biotin at 4 °C for 45 min. *E*, σ_1R antagonist CM304 blocked the effects of PRE-084 on cocaine-induced accessibility changes of Cys-306 in DAT. Cells were incubated with CM304 for 15 min before PRE-084 treatment for 1 h at 37 °C with CM304 also present. *F*, potentiation of cocaine-induced accessibility changes of T316C/C306A DAT by σ_1R agonists. All *bar graphs* (*B–F*) show summarized results (mean ± S.E.) from multiple experiments (*n*) with representative immunoblots of labeled DAT and lysate DAT signals. *, $p < 0.05$; ***, $p < 0.001$, one-way ANOVA with post-hoc Bonferroni's multiple comparison test. *NS*, not significant. *(+)pent*, (+)-pentazocine.

were examined for interaction with DAT in transfected cells, both exhibited stronger association than the full-length (*FL*) σ_1R, whereas σ_1R-xs showed the strongest interaction with DAT (Fig. 3*D*). These surprising results suggested that the interaction between DAT and σ_1R was likely mediated by the TM of σ_1R, as deletion of its cytoplasmic domain did not impair but, instead, enhanced DAT-σ_1R association.

We previously studied conformational changes of DAT using cysteine accessibility assays. Upon cocaine binding, the conformation of DAT was changed so that several residues exhibited altered accessibility, including cysteine 306 (Cys-306) and threonine 316 (Thr-316) on TM6a (Fig. 4*A*), a key domain forming a part of the extracellular vestibule in the outward-facing conformation of DAT (26). To understand why preincubation with σ_1R agonists increased cocaine binding (Fig. 2), we examined whether σ_1R drugs could modulate the DAT conformation. In HEK293 cells co-transfected with wild-type DAT and Myc-tagged σ_1R, exposure of 1 μM cocaine substantially increased the accessibility of Cys-306 (253 ± 29%, mean ± S.E., compared with vehicle), as probed by maleimide-PEG2-biotin, a sulfhydryl-specific, membrane-impermeant reagent. Preincubation with PRE-084 increased the cocaine-induced effects in a dose-dependent manner, with 10 μM PRE-084 producing a significant enhancement to 364 ± 36% of vehicle (Fig. 4*B*).

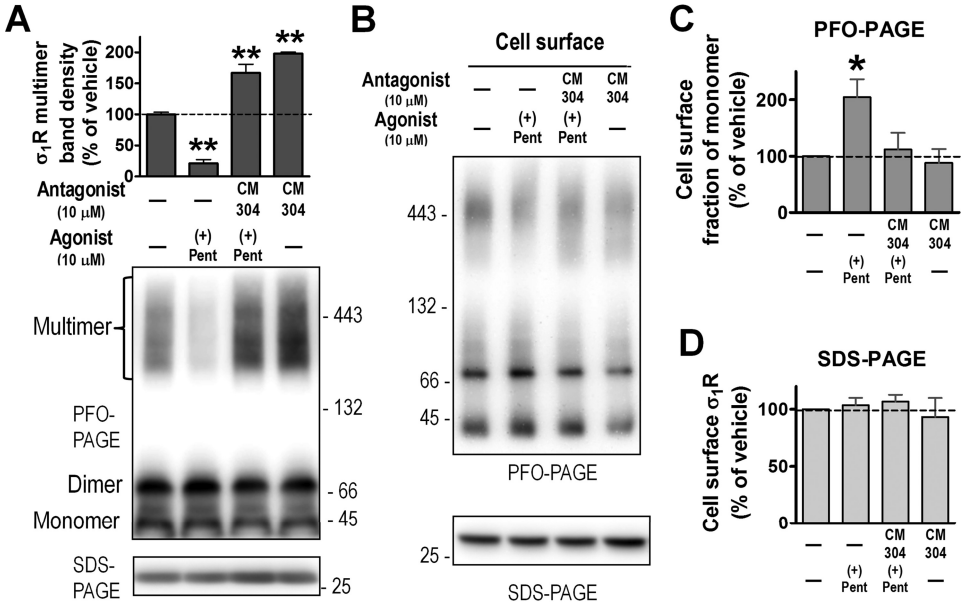

Figure 5. Effects of σ_1R ligands on σ_1R multimerization. *A*, cells expressing FH-σ_1R were incubated with ligands in culture medium at 37 °C for 1 h, then lysed with GDN lysis buffer and subjected to PFO-PAGE. FLAG antibodies detected multiple bands, corresponding to monomer, dimer, and high-order oligomers of σ_1R. Shown are quantified results of multimeric band signals (mean ± S.E., $n = 3$ experiments) with a representative blot. **, $p < 0.01$, one way ANOVA and post-hoc Dunnett's test, compared with vehicle. *B*, after ligand incubation, FH-σ_1R cells were surface biotinylated with sulfo-NHS-biotin at 4 °C. Biotinylated proteins from GDN lysates of cells were enriched with NeutrAvidin beads, separated in PFO-PAGE or SDS-PAGE, and immunoblotted with FLAG antibody (representative blots shown). *C*, cell surface FH-σ_1R bands from PFO-PAGE were quantified. The fraction of monomer out of total signals (including monomer, dimer, and multimer) in each treatment was calculated and normalized to that of vehicle. (+)-Pentazocine significantly increased monomeric FH-σ_1R fractions (mean ± S.E., $n = 4$ experiments). *, $p < 0.05$, one way ANOVA and post-hoc Dunnett's test, compared with vehicle. *D*, cell surface FH-σ_1R bands from SDS-PAGE were quantified. Drug treatment did not significantly alter the overall amount of FH-σ_1R on the cell surface (mean ± S.E., $n = 4$ experiments).

Similarly, 10 μM (+)-pentazocine enhanced cocaine-induced changes in Cys-306 accessibility from 273 ± 20% to 349 ± 29% of vehicle treatment (Fig. 4*C*). However, neither PRE-084 nor (+)-pentazocine pretreatment significantly altered Cys-306 accessibility in the absence of cocaine (Fig. 4, *B* and *C*). Moreover, neither σ_1R agonists changed the cell-surface expression levels of DAT, as measured by cell-surface biotinylation using sulfo-NHS-SS-biotin, a membrane-impermeant probe that selectively reacts with primary amine moieties in proteins (Fig. 4*D*).

Pretreatment with 2 μM CM304, a novel antagonist with subnanomolar affinity and a high selectivity for σ_1R (27, 28), effectively blocked the potentiating effects of 10 μM PRE-084 (Fig. 4*E*), verifying that these effects were mediated specifically through σ_1R. CM304 alone did not alter cocaine-induced changes in Cys-306 accessibility on DAT.

We then probed the cysteine accessibility at a position in closer proximity to the inhibitor-binding pocket of DAT, using a substituted cysteine construct T316C/C306A in which Thr-316 and Cys-306 were mutated to cysteine and alanine, respectively. In cells co-transfected with T316C/C306A DAT and Myc-tagged σ_1R, cocaine binding significantly increased T316C thiol side-chain reactivity toward maleimide-PEG2-biotin to 387 ± 22% of vehicle (Fig. 4*F*). The effect of cocaine was significantly enhanced after preincubation with 20 μM (+)-pentazocine or PRE-084 to 487 ± 26% or 548 ± 49%, respectively (Fig. 4*F*). As in Fig. 4, *B* and *C*, neither PRE-084 nor (+)-pentazocine altered T316C accessibility in the absence of cocaine (Fig. 4*F*).

Together, these biochemical data indicated that pre-exposure to σ_1R agonists enhanced cocaine-induced conformational changes of DAT, suggesting that the interaction with σ_1R likely shifted the conformational equilibrium of DAT toward the outward-facing state which preferentially binds cocaine.

Because σ_1R agonists did not directly alter DAT conformation or its cell-surface expression levels, their modulatory effects on DAT conformation are most likely mediated by σ_1R-DAT interactions. The crystal structure of σ_1R showed a homotrimeric assembly (17). Each monomer has a single TM and a cytoplasmic portion comprising a ligand-binding pocket and trimerization interface. Because oligomerization of membrane proteins may regulate their function, we devised a novel biochemical method to detect σ_1R multimerization. HEK293 cells were transfected with σ_1R containing N-terminal FLAG-2 × His_8 tag (FH-σ_1R), which has a predicted M_r of 32 kDa (25 kDa σ_1R + 7 kDa tags with linker). After incubation with σ_1R ligands, cells were solubilized using a mild detergent, glycodiosgenin (GDN), and electrophoretically separated under non-denaturing conditions using another mild detergent, perfluorooctanoic acid (PFO). FLAG antibodies detected immunoreactive signals of two lower M_r bands (~40 and 70 kDa) and high-M_r diffused bands (>150 kDa), likely corresponding in apparent M_r to the σ_1R monomer, dimer, and oligomer (possibly larger than trimer). Compared with vehicle, the agonist (+)-pentazocine significantly decreased, whereas the antagonist CM304 significantly increased signals of σ_1R oligomers (Fig. 5*A*), suggesting that ligand binding to σ_1R has distinct effects on the multimeric states of σ_1R. When GDN lysates of FH-σ_1R were run under denaturing conditions in SDS-PAGE, only one band (~30 kDa) was seen, similar to σ_1R signals in Fig. 3, *A* and *B*.

Because cell surface DAT is vital in its function, and σ_1R can interact with glycosylated DAT, which is likely in the plasma membrane (Fig. 3, *A* and *D*), we further examined the multimeric status of σ_1R on the cell surface. The FLAG epitope (DYKDDDDK) and enterokinase cleavage sequence (DDDDK) in FH-σ_1R has three lysine residues whose primary amine side chain can react with sulfo-NHS-biotin, a membrane-impermeant cell-surface biotinylation reagent. FH-σ_1R-expressing cells were treated with σ_1R ligands at 37 °C for 1 h in culture medium, washed with cold PBSCM (PBS containing 0.10 mM $CaCl_2$, 1.0 mM $MgCl_2$, pH 7.1), and biotinylated at 4 °C. After cell lysis with GDN, biotinylated proteins were enriched with NeutrAvidin beads, then eluted with sample buffer containing 4% PFO to preserve the multimeric states of σ_1R. Although the majority of σ_1R was intracellular, a portion of σ_1R was present on the cell surface and labeled by sulfo-NHS-biotin. In PFO-PAGE three different bands (~40, ~70, and >150 kDa) of FH-σ_1R were observed, likely corresponding to the monomer, dimer, and multimer (Fig. 5*B*). With (+)-pentazocine pretreatment, the fraction of σ_1R monomers on the cell surface was significantly increased compared with vehicle (Fig. 5*C*). However, if the NeutrAvidin beads PFO eluates were then incubated with SDS sample buffer and run in SDS-PAGE, only one band of ~30 kDa was seen, which represented the denatured σ_1R monomer derived from monomer, dimer, and multimer under native conditions. No statistical difference in σ_1R band densities in SDS-PAGE was seen with σ_1R drug treatment (Fig. 5*D*). These results demonstrate that (+)-pentazocine does not change the overall amount of FH-σ_1R on the cell surface but specifically alters its quaternary organization to induce more monomer formation.

Discussion

In the present study we explored molecular mechanisms underlying behavioral potentiation of cocaine self-administration by σ_1R agonists. Our data in native tissues and transfected cells show that pretreatment of σ_1R agonists shifts DAT conformation toward an outward-facing conformation (Fig. 4), which facilitates cocaine binding (Fig. 2) and enhances cocaine self-administration potency (Fig. 1). Furthermore, σ_1R agonists did not directly affect DAT conformation or cell-surface expression levels but likely exert their effects by altering multimeric states of σ_1R, thus modulating its dynamic interaction with DAT. The agonist (+)-pentazocine dissociated σ_1R multimers to monomers and dimers (Fig. 5) and potentiated cocaine-induced changes in DAT conformation (Fig. 4), whereas the antagonist CM304 had the opposite effects on σ_1R oligomerization and no effects on DAT conformation. Taken together, our results support the hypothesis that the dissociation of σ_1R multimers to monomers by σ_1R agonists facilitates the interaction of σ_1R with DAT and promotes an outward-facing conformation of DAT, thus enhancing cocaine binding and potentiating the response to cocaine (Fig. 6).

The transport cycle of DAT involves coordinated movement of key domains that enables DAT to switch between the outward-facing and inward-facing conformations. Pharmacological studies (26, 29) and recent atomic structures of *Drosophila* DAT (7) have confirmed that cocaine binds to DAT in the outward-facing conformation. Based on biochemical, pharmacological and behavioral data presented in this study, we speculate that interaction with σ_1R shifts the DAT conformation toward an outward-facing state in which cocaine binding is facilitated, although detailed molecular mechanisms involved in such modulation requires further elucidation. Our cysteine accessibility assays were optimized to examine cocaine-induced conformational changes of DAT at Cys-306 and T316C, but they did not detect significant effects of σ_1R agonists in the absence of cocaine (Fig. 4). It is possible that such modulation may involve conformational changes of other domains on DAT. Because cocaine binding to DAT is promoted by DAT-σ_1R interaction, modulatory effects by σ_1R agonists were eventually unmasked as potentiation of cysteine accessibility changes at Cys-306 or T316C. In other words, conformational changes of DAT induced by cocaine binding are apparently enhanced after σ_1R agonists treatment.

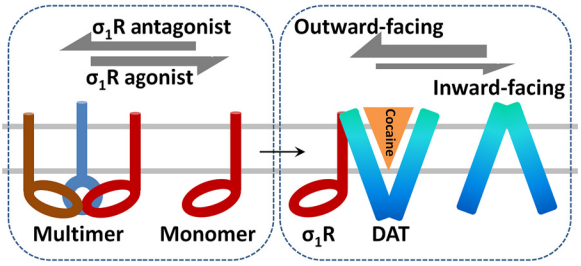

Figure 6. Hypothesis schematic summarizing the modulation of DAT conformation and cocaine binding by σ_1R. Binding of σ_1R agonists facilitates dissociation of σ_1R multimers to monomers, which then dynamically interact with DAT to promote an outward-facing conformation of DAT, thus enhancing cocaine binding and potentiating cocaine's behavioral response.

The σ_1R agonist (+)-pentazocine dose-dependently shifted the cocaine self-administration dose-effect curve to the left (Fig. 1). A similar effect was obtained previously with other σ_1R agonists, PRE-084 and DTG (22). Additionally, the effects of the σ_1R agonists on cocaine self-administration were similar to the effects of DA uptake inhibitors, such as methylphenidate or WIN35428 (22), suggesting that σ_1R agonists may act through DAT to potentiate the reinforcing effects of cocaine. In contrast, σ_1R antagonists at doses effective in blocking σ_1R agonist effects had no effects on cocaine self-administration when administered alone, suggesting a crucial modulatory role of σ_1R on the DA signaling that is critically involved in cocaine self-administration. In the present study we identified a novel modulatory mechanism of σ_1R on DAT, the key element initiating DA signaling due to cocaine administration. Data presented here suggest that the interaction with σ_1R likely stabilizes a conformation of DAT, which is preferable for cocaine binding. This correlates with the observations that lower doses of cocaine were sufficient to produce reinforcing effects, *i.e.* a leftward shift of cocaine dose response.

We previously found that membrane cholesterol promotes the outward-facing conformation of DAT and increases [^{3}H]WIN35428 binding B_{max} in native tissues and transfected cells (26). Indeed, cholesterol has been shown to be associated with *Drosophila* DAT bound with inhibitors such as cocaine in X-ray crystal structures (7, 30). As cholesterol binding hinders the movement of TM1a, which is necessary for DAT to transi-

tion into the inward-facing conformation, it is speculated that cholesterol plays a critical role in stabilizing outward-facing conformation of DAT (30).

Interestingly, the effects of σ_1R agonists on DAT binding resemble those exerted by increasing the membrane cholesterol content. Both treatments increased B_{max} values of [^{3}H]WIN35428 binding (Fig. 2, *B* and *D*) without changing cell-surface expression levels of DAT (Fig. 4*D*). Furthermore, σ_1R has been suggested to bind cholesterol (31) and contain steroid-binding domains like-I and II (32, 33). It is reasonable to speculate that interaction with σ_1R may increase the membrane cholesterol content in the microdomains surrounding DAT proteins, thus shifting the equilibrium of DAT conformation toward the outward-facing direction. This conjecture will require further studies to resolve several important questions. It remains to be elucidated whether cholesterol can occupy the ligand-binding pocket of σ_1R or associate with σ_1R in another manner and how multimeric status of σ_1R can impact its ability to bind cholesterol. Nevertheless, cumulative data from the work reported here and by others appear to support the hypothesis that as a cholesterol carrier σ_1R may interact with and modulate the function of various membrane proteins.

Alternatively, association with σ_1R may affect the quaternary structure of DAT. It is worth noting that high-M_r DAT bands appeared to be preferentially enriched with GST-σ_1R (Fig. 3, *A* and *D*), suggesting direct or indirect association of σ_1R with oligomeric DAT proteins. Earlier studies have shown that DAT likely exists as multimers in native membrane environment (34–37), and its oligomeric states can affect [^{3}H]WIN35428 binding through protomer cooperativity (38). Thus, the dynamic interaction between DAT and σ_1R at molecular levels will require future investigation employing more sophisticated techniques.

A one-TM topology of σ_1R was proposed when it was originally cloned (9). Subsequent studies suggested that σ_1R possessed two TMs (11, 13). Recently the crystal structure of σ_1R showed a homotrimer with each protomer containing a single TM and a cytoplasmic C terminus (17). Our data support this one-TM model, with an extracellular N terminus and a cytoplasmic C terminus when σ_1R is expressed on the cell surface, because N-terminal FLAG-tagged σ_1R was efficiently labeled at lysine residues by the membrane-impermeant sulfo-NHS-biotin (Fig. 5*B*). In addition, a substituted cysteine construct of σ_1R containing W9C at its N terminus was labeled by the membrane-impermeant maleimide-PEG2-Biotin. In contrast, another construct with M170C at its C terminus was not labeled (data not shown).

We devised a novel biochemical method to examine the multimeric status of σ_1R. First, σ_1R-expressing cells were solubilized by GDN, a mild detergent that has been shown to be superior to dodecylmaltoside in stabilizing solubilized membrane proteins (39). Second, GDN-solubilized proteins were electrophoretically separated using buffer containing PFO, another mild detergent shown to preserve the oligomerization status of membrane proteins (40–43). It appeared that, at least in transfected cells, the bulk of the epitope-tagged σ_1R exists as high-order multimers, because only high-M_r bands were observed when GDN lysates were incubated with PFO sample buffer at room temperature. The apparent M_r (>150 kDa) of these bands suggested a quaternary assembly possibly larger than trimers (Fig. 5*A*). This is consistent with results from early purification studies using [^{3}H](+)SKF10047 or [^{3}H]azido-DTG as affinity ligands in which the labeled protein complex under non-denaturing conditions appeared to be >150 kDa (44–46).

High- and low-M_r σ_1R bands were revealed after optimizing the incubation temperature of GDN lysates and PFO sample buffer to 50 °C. Although in non-denaturing gels the migration rate of a protein might not accurately correlate with its M_r as in SDS-PAGE, the apparent M_r (~40 and 70 kDa) of low-M_r bands most likely corresponded to monomeric and dimeric σ_1R. The absence of signals between 70 and ~150 kDa suggested that larger assemblies than trimers were predominant in these cells.

Treatment with (+)-pentazocine or CM304 had opposite effects on the multimeric states of σ_1R (Fig. 5, *A* and *B*). Several agonists or antagonists had effects similar to those of (+)-pentazocine or CM304, respectively.[3] Additionally, differential effects of ligands on σ_1R multimerization were observed using HA- or Myc-tagged σ_1R, ruling out possibly spurious results from the FLAG epitope.[3] These biochemical results are consistent with recent findings that Förster resonance energy transfer signals between cyan or yellow fluorescent protein-tagged σ_1R were decreased by agonist (+)-pentazocine but increased by antagonist haloperidol in transfected cells (47). It has also been reported that multimeric states of purified σ_1R in detergent micelles were stabilized by some ligands (48).

Our biochemical data indicate that through direct or indirect manners σ_1R associates with unglycosylated, glycosylated, and oligomeric DAT (Fig. 3, *A* and *D*), suggesting their interactions occur in various intracellular compartments and on the plasma membrane. Although the majority of σ_1R reside on the ER, we detected the presence of σ_1R in the plasma membrane using cell-surface biotinylation assays (Fig. 5*B*). Furthermore, there were distinct effects of σ_1R agonists or antagonists on multimeric states of σ_1R on the cell surface (Fig. 5*C*). It is plausible that the portion of σ_1R in the plasma membrane plays a more important role in modulating the function of various interacting membrane proteins such as the channels and receptors identified so far and the DAT in this study. We hypothesize that σ_1R agonists promote σ_1R-DAT interactions by increasing σ_1R monomers. Previous studies employing atomic force microscopy have demonstrated that σ_1R associates with a trimeric acid-sensing channel with 3-fold symmetry (49) and with a tetrameric sodium channel with 4-fold symmetry (50). Although we cannot rule out the possibility that DAT associates with oligomeric σ_1R, such interactions may be energetically unfavorable due to steric hindrance. Furthermore, the σ_1R-xs splice variant, which retains the TM sequence but lacks cytoplasmic ligand binding and trimerization domains, exhibited stronger association with DAT (Fig. 3*D*). Therefore, current data favor the model that σ_1R monomers preferentially interact with DAT.

In summary, in this study we present biochemical, pharmacological, and behavioral evidence to demonstrate that σ_1R

[3] W. C. Hong, manuscript in preparation.

interacts with DAT and modulates DAT function. Our data support the hypothesis that agonists of σ_1R affect its oligomerization and interaction with DAT, inducing an outward-facing conformation of DAT and facilitating cocaine binding to DAT. This study represents a first step to decipher the mechanisms underlying potentiation of cocaine self-administration by σ_1R agonists, although further work is necessary to fully elucidate the molecular and cellular underpinnings of these neural adaptations. As σ_1R ligands have been shown to indirectly modulate DA signaling, exploration of their therapeutic potentials may open a new avenue in treating cocaine addiction.

Experimental procedures

Chemicals, radioligands, and antibodies

Sources of reagents are as follows: (−)-cocaine HCl, (+)-pentazocine succinate, WIN35428, National Institute on Drug Abuse (NIDA) Drug Supply Program; PRE-084, Tocris (Minneapolis, MN); maleimide-PEG2-biotin, sulfo-NHS-SS-biotin, sulfo-NHS-biotin, NeutrAvidin-agarose beads, BCA protein kit, Pierce; [^{3}H]DA (NET673, 16.9 to 30.6 Ci/mmol) and [^{3}H]WIN35428 (NET1033, 85.9 Ci/mmol), PerkinElmer Life Sciences; PFO, TCI America (Portland, OR); GDN, Anatrace (Maumee, OH); all other chemicals, Sigma or Fisher. Antibodies were from: anti-DAT MAB369, Chemicon (Temecula, CA); rabbit antisera against DAT N terminus (26); σ_1R rabbit antisera (Su laboratory); anti-Myc 9E10 mAb, protein A/G beads, Santa Cruz Biotechnology (Santa Cruz, CA); anti-FLAG rat mAb L5, anti-GST rabbit poly9248, Biolegend (San Diego, CA); glutathione-conjugated Sepharose beads, GE Healthcare; HRP-conjugated secondary antibodies, Biolegend or Jackson ImmunoResearch (West Grove, PA).

Behavioral pharmacology

Adult male Sprague-Dawley rats (Taconic Farms, Germantown, NY) were surgically prepared with indwelling venous catheters and trained to self administer cocaine under a fixed-ratio (FR) five-response schedule of reinforcement in standard operant conditioning chambers using previously described methods (51). Experimental sessions were conducted daily with subjects enclosed within chambers containing two response levers (with stimulus lights above each) and a food tray. The catheter was attached via tubing to an external infusion pump via a ceiling-mounted swivel. After recovery from surgery, subjects were allowed to self administer cocaine (0.32 mg/kg/injection, intravenous) and trained over a series of sessions. Under the final conditions the emission of 5 responses produced a cocaine injection during 20-min components of the session separated by 2-min timeout periods in which cocaine was not available. Unit dose of cocaine increased from 0 mg/kg/injection in the first component to 1.0 mg/kg/injection in the fifth component. Test sessions before which σ_1R agonists were administered were interspersed between training sessions and separated by a minimum of 72 h. The response rates were calculated by dividing the total responses by the elapsed time during components, excluding responses and time during time-out periods. Med Associates Inc. (St. Albans, VT) software was used to control the experiments and to create cumulative records of responding. Effects on response rates were assessed by ANOVA, with post hoc Tukey tests using SigmaPlot software (Systat Software, Inc., San Jose, CA) with statistical significance set at $p < 0.05$.

Radioligand binding assay

Male Sprague-Dawley rats (150–250 g, Charles River) were euthanized, and striatal tissues were dissected immediately. Tissues were quickly rinsed with artificial cerebrospinal fluid (aCSF, 125 mM NaCl, 2.5 mM KCl, 1.25 mM NaH_2PO_4, 1 mM $MgCl_2$, 26 mM $NaHCO_3$, 11 mM glucose, 2.4 mM $CaCl_2$) and then chopped into 0.5-mm slices using a McIlwain tissue chopper, washed 3 times with aCSF, and divided into approximately equal portions in 20 ml of aCSF containing σ_1R ligands or vehicle. Tissues were incubated at 35 °C with continuous oxygenation for 1 h and then washed 3 times with ice-cold sucrose-phosphate buffer (SPB, 0.32 M sucrose, 7.74 mM Na_2HPO_4, 2.26 mM NaH_2PO_4, pH 7.4). Afterward tissues were resuspended in 5 ml of SPB, homogenized using a Brinkman Polytron, and centrifuge at 10,000 × *g* for 10 min at 4 °C. The pellet was resuspended in 5 ml of SPB and centrifuged again at 10,000 × *g* for 10 min at 4 °C. The resulting pellet was resuspended in 5 ml of SPB and divided into 0.2-ml aliquots in glass test tubes. Aliquots were also saved for measuring protein concentrations. The binding reactions were initiated by adding competing ligands and 0.5 nM [^{3}H]WIN35428 in a total volume of 0.5 ml, then incubated on ice for 2 h and terminated by rapid filtration through Whatman GF/B filters (presoaked in 0.05% polyethyleneimine (PEI)) using a cell harvester (Brandel Instruments, Gaithersburg, MD). The filters were washed twice with 5.0 ml of cold buffer, soaked with scintillation mixture overnight, and measured for radioactivity using a Tri-Carb 2910TR liquid scintillation counter (PerkinElmer Life Sciences) at 50% efficiency. Nonspecific binding measured in the presence of 100 μM cocaine was subtracted from total counts to obtain specific binding. Data were analyzed using GraphPad Prism (San Diego, CA) for non-linear regression to derive B_{max} and K_i values. All animal-related protocols were approved by the National Institute on Drug Abuse Intramural Research Program Animal Care and Use Committee.

DNA subcloning and stable expression cell lines

The coding sequences of human DAT or human σ_1R cDNA were subcloned into CMV promoter-based mammalian expression vectors: pcDNA3.1(+) (Invitrogen), pCMV-tag5A (Stratagene, La Jolla, CA), or plasmids expressing N-terminal fusion of Myc, HA, GST, or FLAG-2 × His_8 tags that were custom-made in the laboratory and verified by standard DNA sequencing procedures. Plasmids were linearized with PvuI, MluI, or ApaL1 and transfected into HEK293 cells with TransIT LT1 reagent (Mirus Bio, Madison, WI). Cells were then cultured in DMEM (Sigma) with 10% FBS (Invitrogen), penicillin-streptomycin, and 0.5 mg/ml G418 in humidified incubators with 5% CO_2 at 37 °C. Expression of DAT and σ_1R in G418-resistant pools or clones was verified by immunoblot using antibodies against DAT, σ_1R, or epitope tags. To overcome potential limitations of cell-line specific effects, multiple lines of HEK293 cells were constructed to stably co-express DAT

and σ_1R. The following cell lines were used in uptake, binding, or cysteine accessibility assays, including "D-S" (expressing DAT + σ_1R), "D-SM" (DAT + C-Myc-tagged σ_1R), "HD-MS" (HA-tagged DAT + N-Myc tagged σ_1R), and "T316C-MS" (T316C/C306A DAT + N-Myc tagged σ_1R).

[^{3}H]DA uptake and [^{3}H]WIN35428 binding in transfected cells

D-S cells were seeded into PEI-coated 96-well plates and cultured to confluency. After cultured medium was aspirated using an ELx50 plate washer (BioTek, Winooski, VT), cells were washed twice and then incubated in low-Na^+ buffer (NaCl 50 mM, 100 mM *N*-methyl-D-glucamine, 2 mM KCl, 1 mM $CaCl_2$, 1 mM $MgCl_2$, 5 mM glucose, 5 mM HEPES, pH 7.4) for 2 h at 37 °C in the absence or presence of σ_1R ligands.

For uptake assays, after drug incubation cells were washed twice and then incubated at room temperature for 5 min with 100 μl of low-Na^+ buffer containing 25 nM [^{3}H]DA and various concentrations of unlabeled DA and 5 μM catechol-*O*-methyl transferase inhibitor Ro 41–0960. Cells were then washed with cold PBSCM using a plate washer and lysed with 0.2 ml of scintillation mixture overnight. Retained radioactivity was determined by a Wallac MicroBeta2 liquid scintillation counter (PerkinElmer Life Sciences). Data were analyzed using the Michaelis-Menten kinetic equation with GraphPad Prism.

For binding assays, after drug incubation D-S cells or HD-MS cells were then washed twice and incubated with low-Na^+ buffer containing 7.5 nM [^{3}H]WIN35428 and various concentrations of unlabeled WIN35428 at 4 °C for 1.5 h. Cells were then washed with cold PBSCM using a plate washer, and bound radioactivity was determined as described above. Data were analyzed with GraphPad Prism for non-linear curve-fitting.

Co-immunoprecipitation and GST pulldown

HEK293 cells in 60-mm culture dishes were transfected to co-express GST-σ_1R and Myc-σ_1R, DAT, or EAAT2. Two days after transfection, cells were collected and incubated with TNE lysis buffer (1% Triton X-100, NaCl 150 mM, EDTA 1 mM, Tris 10 mM, pH 7.5, and protease inhibitors) at 4 °C for 1 h followed by centrifugation at 18,000 × *g* for 20 min at 4 °C. Aliquots of the supernatants were saved as lysate input and for protein concentration measurement; the remaining portions were incubated with 40 μl of 50% slurry of glutathione-conjugated Sepharose beads (prewashed with TNE buffer) on a rotator for 4 h at 4 °C. After washing beads three times with TNE lysis buffer, proteins were eluted with SDS sample buffer and separated by SDS-PAGE, transferred to PVDF membranes, and detected by immunoblotting and chemiluminescence methods.

Confluent D-S cells in 60-mm culture dishes were incubated with TNE lysis buffer at 4 °C for 1 h and centrifugation at 18,000 × *g* for 20 min at 4 °C. Supernatants were incubated with 1 μg of anti-DAT MAB369 (rat mAb) or normal rat IgG at 4 °C for 2 h followed by the addition of 40 μl of protein A/G beads and incubated for 2 h. Afterward beads were washed three times with TNE lysis buffer. Proteins were eluted and detected as described above.

BRET assays

The cDNAs encoding *Renilla* luciferase (RLuc) or monomeric Venus were fused in-frame to the C terminus of σ_1R and N terminus of DAT or EAAT2 in the pcDNA3.1 vector. The BRET assays were performed as described previously (52). Briefly, HEK293T cells were transfected using a constant amount of plasmid DNA but various ratios of plasmids encoding the fusion protein partners. A control corresponding to mock-transfected cells was included in order to subtract raw basal luminescence and fluorescence from the data. Expression of monomeric Venus fusion proteins was estimated by measuring fluorescence at 535 nm after excitation at 485 nm. Expression of RLuc fusion proteins was estimated by measuring the luminescence of the cells after incubation with 5 μM coelenterazine-h. In parallel, BRET was measured as the fluorescence of the cells at 535 nm at the same time points using a Mithras LB940 reader (Berthold Technologies, Bad Wildbad, Germany).

DAT cysteine accessibility assays and cell-surface biotinylation

D-SM cells or T316C-MS cells were seeded into PEI-coated 6-well or 12-well plates and cultured to confluency. Cells were washed 3 time with PBSCM + 10 mM glucose (PBSCMG) and then incubated with σ_1R ligands in PBSCMG at 37 °C for 1 h. Afterward cells were washed 3 times with cold PBSCM, then incubated with 0.5 mg/ml maleimide-PEG2-biotin in the presence or absence of cocaine for 45 min at 4 °C with gentle shaking. The labeling reaction was quenched with PBSCM containing 2 mM DTT or 50 mM cysteine for 15 min at 4 °C. Cells were then washed, harvested, and lysed in TNE lysis buffer for 1 h at 4 °C followed by a 20-min centrifugation at 18,000 × *g*. Aliquots of supernatants were saved for protein concentration measurement. Remaining supernatants were incubated with 60 μl of NeutrAvidin-agarose beads overnight at 4 °C. After washing beads three times with TNE buffer, biotinylated proteins were eluted with SDS sample buffer, separated by SDS-PAGE, transferred to PVDF membranes, and probed with MAB369 or rabbit antisera for DAT. Chemiluminescent signals were captured with a MultiImage III device (Alpha Innotech, San Leandro, CA) as digital TIFF images without pixel saturation. Mean densities of DAT bands were quantified using the NIH ImageJ software and normalized to percent of vehicle. DAT or σ_1R expression levels on the cell surface were measured by procedures similar to those outlined above, except that cells were incubated with 0.5 mg/ml sulfo-NHS-SS-biotin or sulfo-NHS-biotin in PBSCM at 4 °C for 45 min followed by quenching with 100 mM glycine.

Analysis of σ_1R multimeric states by PFO-PAGE

Confluent FH-σ_1R cells in 12-well plates were incubated with σ_1R ligands at 37 °C for 1 h in culture medium. Cells were then washed with cold PBSCM, harvested, and incubated with lysis buffer (0.1% GDN, NaCl 150 mM, EDTA 1 mM, Tris 10 mM, pH 7.5, and protease inhibitors) for 1 h at 4 °C. After lysates were centrifuged at 20,000 × *g* for 20 min, supernatants were mixed with an equal volume of 2× PFO sample buffer (8% PFO, 40% glycerol, bromphenol blue 0.005%, Tris 100 mM, pH 7.5) to a final concentration of 4% PFO and heated at 50 °C for 10 min.

Samples were run in 5–15% polyacrylamide Tris-glycine gels (running buffer: 0.1% PFO, 25 mM Tris, 192 mM glycine, pH 8.3). Proteins were transferred to PVDF membranes and immunoblotted with rat monoclonal anti-FLAG L5 antibodies. Because commercial protein markers containing SDS were not suitable in this system, the following proteins were mixed with PFO sample buffer and used as molecular standards: egg white lysozyme (14 kDa), ovalbumin (45 kDa), BSA (66 kDa monomer, 132-kDa dimer), and equine apoferritin (443 kDa).

Author contributions—W. C. H. designed, conducted, and analyzed the experiments in Figs. 2–5 and wrote most of the paper. T. H. and J. L. K. designed, performed, and analyzed the experiments Fig.1. H. Y. designed, conducted, and analyzed the experiments in Fig. 3. C. R. M. and F. T. C. provided novel reagents. S. G. A., T.-P. S., and all other authors contributed to designing experiments, reviewing the results, and writing the paper. All approved the final version of the manuscript.

Acknowledgments—The National Institute on Drug Abuse Drug Supply Program kindly provided (−)-cocaine HCl, (+)-pentazocine succinate, and WIN35428. We thank Dr. Linda Werling for providing human σ_1R cDNA and critical reading of this manuscript.

References

1. Amara, S. G., and Kuhar, M. J. (1993) Neurotransmitter transporters: recent progress. *Annu. Rev. Neurosci.* **16,** 73–93
2. Sulzer, D., Cragg, S. J., and Rice, M. E. (2016) Striatal dopamine neurotransmission: regulation of release and uptake. *Basal Ganglia* **6,** 123–148
3. German, C. L., Baladi, M. G., McFadden, L. M., Hanson, G. R., and Fleckenstein, A. E. (2015) Regulation of the dopamine and vesicular monoamine transporters: pharmacological targets and implications for disease. *Pharmacol. Rev.* **67,** 1005–1024
4. Kristensen, A. S., Andersen, J., Jørgensen, T. N., Sørensen, L., Eriksen, J., Loland, C. J., Strømgaard, K., and Gether, U. (2011) SLC6 neurotransmitter transporters: structure, function, and regulation. *Pharmacol. Rev.* **63,** 585–640
5. Vaughan, R. A., and Foster, J. D. (2013) Mechanisms of dopamine transporter regulation in normal and disease states. *Trends Pharmacol. Sci.* **34,** 489–496
6. Bermingham, D. P., and Blakely, R. D. (2016) Kinase-dependent regulation of monoamine neurotransmitter transporters. *Pharmacol. Rev.* **68,** 888–953
7. Wang, K. H., Penmatsa, A., and Gouaux, E. (2015) Neurotransmitter and psychostimulant recognition by the dopamine transporter. *Nature* **521,** 322–327
8. Martin, W. R., Eades, C. G., Thompson, J. A., Huppler, R. E., and Gilbert, P. E. (1976) The effects of morphine- and nalorphine- like drugs in the nondependent and morphine-dependent chronic spinal dog. *J. Pharmacol. Exp. Ther.* **197,** 517–532
9. Hanner, M., Moebius, F. F., Flandorfer, A., Knaus, H. G., Striessnig, J., Kempner, E., and Glossmann, H. (1996) Purification, molecular cloning, and expression of the mammalian sigma1-binding site. *Proc. Natl. Acad. Sci. U.S.A.* **93,** 8072–8077
10. Hayashi, T., and Su, T. P. (2001) Regulating ankyrin dynamics: Roles of sigma-1 receptors. *Proc. Natl. Acad. Sci. U.S.A.* **98,** 491–496
11. Aydar, E., Palmer, C. P., Klyachko, V. A., and Jackson, M. B. (2002) The sigma receptor as a ligand-regulated auxiliary potassium channel subunit. *Neuron* **34,** 399–410
12. Kourrich, S., Hayashi, T., Chuang, J. Y., Tsai, S. Y., Su, T. P., and Bonci, A. (2013) Dynamic interaction between sigma-1 receptor and Kv1.2 shapes neuronal and behavioral responses to cocaine. *Cell* **152,** 236–247
13. Hayashi, T., and Su, T. P. (2007) Sigma-1 receptor chaperones at the ER-mitochondrion interface regulate Ca^{2+} signaling and cell survival. *Cell* **131,** 596–610
14. Navarro, G., Moreno, E., Aymerich, M., Marcellino, D., McCormick, P. J., Mallol, J., Cortés, A., Casadó, V., Canela, E. I., Ortiz, J., Fuxe, K., Lluís, C., Ferré, S., and Franco, R. (2010) Direct involvement of sigma-1 receptors in the dopamine D1 receptor-mediated effects of cocaine. *Proc. Natl. Acad. Sci. U.S.A.* **107,** 18676–18681
15. Navarro, G., Moreno, E., Bonaventura, J., Brugarolas, M., Farré, D., Aguinaga, D., Mallol, J., Cortés, A., Casadó, V., Lluís, C., Ferre, S., Franco, R., Canela, E., and McCormick, P. J. (2013) Cocaine inhibits dopamine D2 receptor signaling via sigma-1-D2 receptor heteromers. *PLoS ONE* **8,** e61245
16. Kim, F. J., Kovalyshyn, I., Burgman, M., Neilan, C., Chien, C. C., and Pasternak, G. W. (2010) Sigma 1 receptor modulation of G-protein-coupled receptor signaling: potentiation of opioid transduction independent from receptor binding. *Mol. Pharmacol.* **77,** 695–703
17. Schmidt, H. R., Zheng, S., Gurpinar, E., Koehl, A., Manglik, A., and Kruse, A. C. (2016) Crystal structure of the human sigma1 receptor. *Nature* **532,** 527–530
18. Walker, J. M., Bowen, W. D., Walker, F. O., Matsumoto, R. R., De Costa, B., and Rice, K. C. (1990) Sigma receptors: biology and function. *Pharmacol. Rev.* **42,** 355–402
19. Gonzalez-Alvear, G. M., and Werling, L. L. (1994) Regulation of [^{3}H]dopamine release from rat striatal slices by sigma receptor ligands. *J. Pharmacol. Exp. Ther.* **271,** 212–219
20. Narayanan, S., Mesangeau, C., Poupaert, J. H., and McCurdy, C. R. (2011) Sigma receptors and cocaine abuse. *Curr. Top. Med. Chem.* **11,** 1128–1150
21. Robson, M. J., Noorbakhsh, B., Seminerio, M. J., and Matsumoto, R. R. (2012) Sigma-1 receptors: potential targets for the treatment of substance abuse. *Curr. Pharm. Des.* **18,** 902–919
22. Hiranita, T., Soto, P. L., Tanda, G., and Katz, J. L. (2010) Reinforcing effects of sigma-receptor agonists in rats trained to self-administer cocaine. *J. Pharmacol. Exp. Ther.* **332,** 515–524
23. Hiranita, T., Mereu, M., Soto, P. L., Tanda, G., and Katz, J. L. (2013) Self-administration of cocaine induces dopamine-independent self-administration of sigma agonists. *Neuropsychopharmacology* **38,** 605–615
24. Katz, J. L., Hong, W. C., Hiranita, T., and Su, T. P. (2016) A role for sigma receptors in stimulant self-administration and addiction. *Behav. Pharmacol.* **27,** 100–115
25. Kourrich, S., Su, T. P., Fujimoto, M., and Bonci, A. (2012) The sigma-1 receptor: roles in neuronal plasticity and disease. *Trends Neurosci.* **35,** 762–771
26. Hong, W. C., and Amara, S. G. (2010) Membrane cholesterol modulates the outward facing conformation of the dopamine transporter and alters cocaine binding. *J. Biol. Chem.* **285,** 32616–32626
27. James, M. L., Shen, B., Zavaleta, C. L., Nielsen, C. H., Mesangeau, C., Vuppala, P. K., Chan, C., Avery, B. A., Fishback, J. A., Matsumoto, R. R., Gambhir, S. S., McCurdy, C. R., and Chin, F. T. (2012) New positron emission tomography (PET) radioligand for imaging sigma-1 receptors in living subjects. *J. Med. Chem.* **55,** 8272–8282
28. Katz, J. L., Hiranita, T., Kopajtic, T. A., Rice, K. C., Mesangeau, C., Narayanan, S., Abdelazeem, A. H., and McCurdy, C. R. (2016) Blockade of cocaine or sigma receptor agonist self-administration by subtype-selective sigma receptor antagonists. *J. Pharmacol. Exp. Ther.* **358,** 109–124
29. Reith, M. E., Berfield, J. L., Wang, L. C., Ferrer, J. V., and Javitch, J. A. (2001) The uptake inhibitors cocaine and benztropine differentially alter the conformation of the human dopamine transporter. *J. Biol. Chem.* **276,** 29012–29018
30. Penmatsa, A., Wang, K. H., and Gouaux, E. (2013) X-ray structure of dopamine transporter elucidates antidepressant mechanism. *Nature* **503,** 85–90
31. Palmer, C. P., Mahen, R., Schnell, E., Djamgoz, M. B., and Aydar, E. (2007) Sigma-1 receptors bind cholesterol and remodel lipid rafts in breast cancer cell lines. *Cancer Res.* **67,** 11166–11175
32. Fontanilla, D., Hajipour, A. R., Pal, A., Chu, U. B., Arbabian, M., and Ruoho, A. E. (2008) Probing the steroid binding domain-like I (SBDLI) of

the sigma-1 receptor binding site using *N*-substituted photoaffinity labels. *Biochemistry* **47,** 7205–7217
33. Pal, A., Chu, U. B., Ramachandran, S., Grawoig, D., Guo, L. W., Hajipour, A. R., and Ruoho, A. E. (2008) Juxtaposition of the steroid binding domain-like I and II regions constitutes a ligand binding site in the sigma-1 receptor. *J. Biol. Chem.* **283,** 19646–19656
34. Hastrup, H., Karlin, A., and Javitch, J. A. (2001) Symmetrical dimer of the human dopamine transporter revealed by cross-linking Cys-306 at the extracellular end of the sixth transmembrane segment. *Proc. Natl. Acad. Sci. U.S.A.* **98,** 10055–10060
35. Sitte, H. H., and Freissmuth, M. (2003) Oligomer formation by Na^+-Cl-coupled neurotransmitter transporters. *Eur. J. Pharmacol.* **479,** 229–236
36. Sorkina, T., Doolen, S., Galperin, E., Zahniser, N. R., and Sorkin, A. (2003) Oligomerization of dopamine transporters visualized in living cells by fluorescence resonance energy transfer microscopy. *J. Biol. Chem.* **278,** 28274–28283
37. Torres, G. E., Carneiro, A., Seamans, K., Fiorentini, C., Sweeney, A., Yao, W. D., and Caron, M. G. (2003) Oligomerization and trafficking of the human dopamine transporter: mutational analysis identifies critical domains important for the functional expression of the transporter. *J. Biol. Chem.* **278,** 2731–2739
38. Zhen, J., Antonio, T., Cheng, S. Y., Ali, S., Jones, K. T., and Reith, M. E. (2015) Dopamine transporter oligomerization: impact of combining protomers with differential cocaine analog binding affinities. *J. Neurochem.* **133,** 167–173
39. Chae, P. S., Rasmussen, S. G., Rana, R. R., Gotfryd, K., Kruse, A. C., Manglik, A., Cho, K. H., Nurva, S., Gether, U., Guan, L., Loland, C. J., Byrne, B., Kobilka, B. K., and Gellman, S. H. (2012) A new class of amphiphiles bearing rigid hydrophobic groups for solubilization and stabilization of membrane proteins. *Chemistry* **18,** 9485–9490
40. Ramjeesingh, M., Huan, L. J., Garami, E., and Bear, C. E. (1999) Novel method for evaluation of the oligomeric structure of membrane proteins. *Biochem. J.* **342,** 119–123
41. Kedei, N., Szabo, T., Lile, J. D., Treanor, J. J., Olah, Z., Iadarola, M. J., and Blumberg, P. M. (2001) Analysis of the native quaternary structure of vanilloid receptor 1. *J. Biol. Chem.* **276,** 28613–28619
42. Penna, A., Demuro, A., Yeromin, A. V., Zhang, S. L., Safrina, O., Parker, I., and Cahalan, M. D. (2008) The CRAC channel consists of a tetramer formed by Stim-induced dimerization of Orai dimers. *Nature* **456,** 116–120
43. Xu, J., Liu, Y., Yang, Y., Bates, S., and Zhang, J. T. (2004) Characterization of oligomeric human half-ABC transporter ATP-binding cassette G2. *J. Biol. Chem.* **279,** 19781–19789
44. McCann, D. J., and Su, T. P. (1991) Solubilization and characterization of haloperidol-sensitive (+)-[^{3}H]SKF-10,047 binding sites (sigma sites) from rat liver membranes. *J. Pharmacol. Exp. Ther.* **257,** 547–554
45. Kavanaugh, M. P., Tester, B. C., Scherz, M. W., Keana, J. F., and Weber, E. (1988) Identification of the binding subunit of the sigma-type opiate receptor by photoaffinity labeling with 1-(4-azido-2-methyl[6-^{3}H]phenyl)-3-(2-methyl[4,6-^{3}H]phenyl)guanidine. *Proc. Natl. Acad. Sci. U.S.A.* **85,** 2844–2848
46. Schuster, D. I., Arnold, F. J., and Murphy, R. B. (1995) Purification, pharmacological characterization, and photoaffinity labeling of sigma receptors from rat and bovine brain. *Brain Res.* **670,** 14–28
47. Mishra, A. K., Mavlyutov, T., Singh, D. R., Biener, G., Yang, J., Oliver, J. A., Ruoho, A., and Raicu, V. (2015) The sigma-1 receptors are present in monomeric and oligomeric forms in living cells in the presence and absence of ligands. *Biochem. J.* **466,** 263–271
48. Gromek, K. A., Suchy, F. P., Meddaugh, H. R., Wrobel, R. L., LaPointe, L. M., Chu, U. B., Primm, J. G., Ruoho, A. E., Senes, A., and Fox, B. G. (2014) The oligomeric states of the purified sigma-1 receptor are stabilized by ligands. *J. Biol. Chem.* **289,** 20333–20344
49. Carnally, S. M., Johannessen, M., Henderson, R. M., Jackson, M. B., and Edwardson, J. M. (2010) Demonstration of a direct interaction between sigma-1 receptors and acid-sensing ion channels. *Biophys. J.* **98,** 1182–1191
50. Balasuriya, D., Stewart, A. P., Crottès, D., Borgese, F., Soriani, O., and Edwardson, J. M. (2012) The sigma-1 receptor binds to the Nav1.5 voltage-gated Na^+ channel with 4-fold symmetry. *J. Biol. Chem.* **287,** 37021–37029
51. Hiranita, T., Soto, P. L., Newman, A. H., and Katz, J. L. (2009) Assessment of reinforcing effects of benztropine analogs and their effects on cocaine self-administration in rats: comparisons with monoamine uptake inhibitors. *J. Pharmacol. Exp. Ther.* **329,** 677–686
52. Sohy, D., Yano, H., de Nadai, P., Urizar, E., Guillabert, A., Javitch, J. A., Parmentier, M., and Springael, J. Y. (2009) Hetero-oligomerization of CCR2, CCR5, and CXCR4 and the protean effects of "selective" antagonists. *J. Biol. Chem.* **284,** 31270–31279